1 **USE OF RESIDUAL AGRICULTURAL PLASTICS AND CELLULOSE FIBERS FOR**

2 **OBTAINING SUSTAINABLE ECO-COMPOSITES PREVENTS WASTE GENERATION**

3

4 **Authors**

5 Carlos González-Sánchez[a, *], Alvar Martínez-Aguirre[a], Beatriz Pérez-García[a], Joaquín

6 Martínez-Urreaga[b], María U. de la Orden [c], Carmen Fonseca-Valero[d].

7 [a]Department of Chemical Engineering and Environmental Technology, Universidad de

8 Oviedo, Avda. Julián Clavería, 8. 33006-Oviedo, Spain.

9 [b]Department of Industrial and Environmental Chemical Engineering, Universidad

10 Politécnica de Madrid, José Gutiérrez Abascal, 2. 28006-Madrid, Spain.

11 [c]Department of Organic Chemistry I, Universidad Complutense de Madrid, Arcos de

12 Jalón, s/n. 28037-Madrid, Spain.

13 [d]Department of Industrial Chemistry and Polymers, Universidad Politécnica de Madrid,

14 Ronda de Valencia, 3. 28012-Madrid, Spain.

15 * Corresponding author. E-mail address: cgs@uniovi.es.

16   Direct phone: +34 985 103519

List of Acronyms:
AF200 = ALFATEN 200
DSC = Differential Scanning Calorimetry
EVA = Ethylene-Vinyl-Acetate Copolymer
FTIR = Fourier Transform Infrared
LDPE = Low-Density Polyethylene
MAPE = Maleic Anhydride-Modified Polyethylene Copolymer
MFI = Melt Flow Index
OIT = Oxidation Induction Time
RAPF = Residual Agricultural Plastic Films
RCF = Residual Cellulose Fibers
SEM = Scanning Electron Microscopy
UV = Ultraviolet
VA = Vinyl Acetate

1 **ABSTRACT**

2   Crop protection residual plastic films are a growing environmental problem which

3 requires efficient solutions. Their suitability as matrices for obtaining sustainable eco-

4 composites reinforced with industrially-sourced residual natural fibers was investigated

5 in order to boost their recovery and prevent waste generation. The analysis of the

6 studied residual agricultural plastics revealed that they are low density polyethylene still

7 containing significant amounts of ethylene-vinyl acetate (2.5 to 4.5 wt%). A pilot-plant

8 extrusion-compounding technology was applied to a selected recycled plastic from

9 residual agricultural films and the residual cellulose fibers for obtaining the eco-

10 composites. The effects of cellulose-fiber content and a selected maleic anhydride-

11 modified polyethylene coupling agent on the properties and interfacial adhesion of the

12 eco-composites were investigated. By using micromechanical models, scientific data of

13 the intrinsic modulus and strength of the *Eucalyptus Globulus* residual fibers, hitherto

14 scarcely available in literature, were found to be 16.4 GPa and 180 MPa, respectively,

15 thus revealing their suitability as cost-effective reinforcement. Tensile modulus and

16 strength of the eco-composites were up to 667 % and 70 % greater than those of the neat

17 agricultural recycled plastic, the latter due to the enhanced compatibility provided by

18 the ethylene-vinyl acetate found. When the coupling agent was added, tensile and

19 flexural strengths increased up to a maximum of 20.26 MPa and 23.96 MPa,

20 respectively. Property variations were found to be due to the fiber length reduction and

21 the interfacial adhesion improvement caused by the coupling agent as well as to its

22 plasticizing effect. The properties achieved revealed the suitability of the eco-

23 composites for their immediate application in the production of numerous

24 environmentally sustainable and cost-effective end-products from the aforementioned

25 wastes.

1   **Keywords:** Agricultural plastics; Waste prevention; Natural fibers; Cellulose;

2   Composites; Intrinsic properties

3

1. INTRODUCTION

Plastic films used in modern intensive agriculture are turning into a growing environmental issue at the end of their useful life. It would then be very interesting to develop efficient solutions that pay off for the costs associated to their recovery, thus preventing waste generation. Due to the important role of plastic films in the production of a host of vegetables and fruits, the area covered with greenhouse, tunnel and mulch plastic films has been increasing since they were first used (by the late 50´s) (Dept. of Agriculture, Food and Environment of Spain, 2012). Thus, by the year 2009, only in China, the country with the greatest greenhouse area in the world, 1,000,000 ha were covered with greenhouse and tunnel plastic films (Cajaraville et al., 2010). In Europe, the greatest greenhouse area is located in Spain, with more than 60,800 ha of greenhouses by 2012 (Dept. of Agriculture, Food and Environment of Spain, 2012).

At the end of the season or after a few seasons those plastic films must be replaced by new ones. According to the most reliable data available, the European production of virgin agricultural plastic films in 2011 was more than 1.7 Mt, most of them being low density polyethylene (LDPE). However, the recovery rate of agricultural plastics was only about 50 % and the mechanical recycling rate was just around 23 % (Plastics Europe, 2011, 2012).

The high volume of residual agricultural plastic films (RAPF) generated, along with their disposal by the farmers through on-site land filling and subsequent burning, turn them into a challenging environmental issue. Moreover, it must be taken into account that many of these films are heavily contaminated with soil, fertilizers and pesticides (Hussain and Hamid, 2003).

One of the ways tried for minimizing the environmental problem associated to the RAPF has been their incineration under controlled conditions. However, from an

1 environmental and sustainability point of view, the mechanical recycling of agricultural

2 plastic film wastes would be a superior solution to incineration.

3 Thus, it has been reported that it is possible to recycle waste greenhouse films for

4 the same application, producing films with a layer of virgin polyethylene and another

5 one consisting of a blend of recycled polyethylene modified with virgin thermoplastics

6 and other stabilizers (Abdel-Bary et al., 1998). Also, it was shown that the use of

7 additives enables the re-building of polyethylene chains, thus improving mechanical

8 properties of residual plastic films (Scaffaro et al., 2006).

9 Agricultural plastic waste can be also used as matrix for composite materials,

10 mainly reinforced with cellulose fibers. RAPF can show several advantages in this

11 application. As they are designed to withstand intensive sun exposure during long

12 periods of time, agricultural plastic films contain relevant amounts of several additives,

13 such as antioxidants and Ultra-Violet (UV) stabilizers, which might still be present in

14 the RAPF (Hussain and Hamid, 2003). On the other hand, they might also contain

15 ethylene-vinyl-acetate copolymer (EVA) (Abdelmouleh et al., 2007). The presence of

16 the polar vinyl acetate moiety in the waste plastic could be interesting, as it would

17 enhance the compatibility between the non-polar polyethylene matrix and the polar

18 cellulose, thus improving the polyethylene-cellulose interfacial adhesion and hence the

19 composite properties. It would therefore be interesting to study if the RAPF still contain

20 noticeable amounts of EVA, antioxidants and stabilizers, as they could give additional

21 value to the recycled agricultural plastic pellets obtained thereof for being used as

22 matrices in cellulose-reinforced eco-composites.

23 Different cellulosic materials (such as wood flour and cellulose fibers) have been

24 used for enhancing the tensile, flexural and thermal properties of several polymeric

25 matrices, thus giving rise to composite materials with important final applications

1   (Abdelmouleh et al., 2007; Bledzki and Gassan, 1999; de la Orden et al., 2007;

2   González-Sánchez et al., 2008). Among the works done, some recently published ones

3   used softwood cellulose pulp fibers (Sdrobiş et al., 2012) and Doum fibers (Arrakhiz et

4   al., 2013) for reinforcing virgin LDPE. Composites were prepared by batch melt mixing

5   or twin-screw extrusion and the composites tensile modulus and strength achieved were

6   about 0.25-0.48 GPa and 10-11 MPa, respectively.

7   In addition to the low cost, density and energy required for production, the main

8   advantages of the use of cellulose fibers are the worldwide availability of renewable

9   sources from which they can be easily obtained, their biodegradability, the lower

10   abrasion of processing equipment, the lower risk for operators if inhaled and, finally,

11   their CO_2 neutrality should they be incinerated (Bledzki and Gassan, 1999). Moreover,

12   they may enhance the biodegradability of LDPE, thus making more environmentally

13   sustainable composite materials (Sunilkumar et al., 2012).

14   There are large amounts of residual cellulose fibers (RCF) that can be used as

15   reinforcement. For instance, in the world´s main process used for the production of

16   cellulose pulp (the Kraft process), a waste stream containing cellulose fibers is

17   generated especially at the washing stage after the wood cooking. For a big pulp mill

18   (*ca*. 500,000 t/year), around 12 t/day of residual cellulose fibers (with a moisture

19   content of 50 wt%) may be generated, which are difficult to dispose off for this

20   industry.

21   Then, the chance of using these residual cellulose fibers (RCF) as renewable

22   reinforcement for polymeric-matrix eco-composites is of great interest from the

23   environmental and economic points of view. Furthermore, the production of composites

24   from RCF and RAPF may induce social benefits in terms of new jobs.

1   Therefore, this work aims to study the suitability of recycled plastic pellets obtained

2   from residual agricultural plastic films and cellulose fibers as raw materials for

3   composites. For this purpose, the residual materials and the recycled agricultural

4   plastics were characterized. The chemical nature and the presence of additives and EVA

5   copolymer in both RAPF and the recycled plastic pellets obtained thereof were studied

6   by Ultra-Violet (UV) and Fourier Transform Infrared (FTIR) spectroscopic techniques.

7   Melt Flow Indices (MFI), tensile properties, crystallinity degrees and Oxidation

8   Induction Times (OIT), measured by Differential Scanning Calorimetry (DSC), were

9   also determined.

10   An extrusion-compounding technology at pilot-plant scale was applied to the

11   selected recycled agricultural plastic and the RCF in order to obtain cellulose-reinforced

12   composites. The effects of cellulose content (25 to 35 wt% of fibers) on the tensile and

13   flexural properties of composites were determined. 35 wt% was selected as the upper

14   limit because in a previous study it was determined that cellulose contents higher than

15   35 wt% make very difficult the extrusion and injection molding processing of these

16   composites. Also, the effect of the addition of two selected percentages (1.5 and 3 wt%)

17   of a selected maleic anhydride-modified polyethylene (MAPE) coupling agent on the

18   composite properties and the fiber-matrix interfacial adhesion was investigated. In order

19   to achieve a further understanding of composite properties and possibilities of use of the

20   RCF, the reinforcing capability of the residual fibers was estimated through the fitting

21   of experimental results to micromechanical models.

22

23

2. MATERIALS AND METHODS

The materials and reagents, the characterization methods of the raw materials, the method used for preparing the composites and the testing methods used through the work are described in this section.

2.1. Materials and reagents

Three residual agricultural plastic films (RAPF) from greenhouses and other uses, two recycled agricultural plastic pellets obtained from different mixtures of RAPF and one commercial virgin plastic (commonly used in the manufacturing of greenhouse films) were characterized. The three RAPF, supplied in shredded films form by BEFESA Plásticos (Spain), were a whitish translucent 0.08 mm thick film (referred to as R1), a transparent 0.04 mm thick film (referred to as R2) and a yellowish translucent 0.19 mm thick film (referred to as R3). The two recycled agricultural plastic pellets were ALFATEN200^{TM} (referred to as AF200), supplied by BEFESA Plásticos (Spain), and PEBD-IB, supplied by IBACPLAST (Spain). The commercial virgin plastic, supplied in pellet form by REPSOL (Spain), was CA2131A, an LDPE with different additives. The main properties of the recycled plastic pellets, given by the suppliers, are shown in Table 1.

Residual cellulose fibers (RCF), a by-product obtained from the manufacturing of Kraft cellulose pulp, mainly consisting of unbleached *Eucaliptus Globulus* cellulose, were supplied by ENCE-Navia (Spain). They were provided as flakes suitable for their feeding to the extrusion-compounding process used for the composite preparation.

A commercially available maleic anhydride-modified polyethylene copolymer (Licocene PE MA 4351 GR, Clariant Ibérica, Spain) was used as coupling agent for improving the interfacial adhesion between the polyolefinic matrix and fibers. It has an

1   acid number of 43, a density at 23 ºC of 990 kg/m^3 and a viscosity at 140 °C of

2   300 mPa·s, approx.

3   0.3 wt% of the thermal stabilizer Irganox B900 (phenol phosphite type), supplied by

4   Ciba (Spain), was used in order to minimize thermal degradation during melt

5   compounding.

6

7   **2.2. Raw materials characterization**

8   Fourier Transform Infrared (FTIR) and UV spectroscopic techniques were used to

9   characterize the raw materials. The FTIR spectra were obtained with a Mattson 3020

10   FTIR Spectrometer (USA) in transmission mode. Each spectrum was recorded at a

11   resolution of 4 cm^{-1}, with a total of 90 scans. The UV spectra were obtained with a

12   Shimadzu 2401 PC UV-VIS Spectrophotometer (Japan). Sheet specimens for the

13   spectroscopic characterization were obtained as films by compression molding in a hot-

14   plate press (IQAP LAP, Spain) at 140 ºC, using a pressure of 2 MPa for 5 min.

15   Melting point (T_m) and crystallinity were determined using a Mettler-Toledo DSC

16   823e (Switzerland), under nitrogen atmosphere. The thermal program used was: *stage I*,

17   heating from room temperature to 150 ºC; *stage II*, cooling from 150 ºC to -60 ºC at

18   5 ºC/min, *stage III,* heating from 60 ºC to 150 ºC at 20 ºC/min. Thermal properties were

19   determined from the third scan. T_m was given by the maximum of the endothermic

20   melting peak. The degree of crystallinity (X_c) was calculated according to the following

21   equation:

22 $$X_c (\%) = (\Delta H_p)/ (\Delta H)_{100\%} \quad (1)$$

23   being ΔH_p the heat of fusion of the tested sample, and $(\Delta H)_{100\%}$ the heat of fusion for

24   the 100 % crystalline PE. OIT measurements were carried out according to

25   ISO 11357-6 standard.

1   Melt flow indices were measured at 190 ºC, with a 2.16 kg mass, according to

2 ISO 1133-1991 standard, using a DAVENPORT melt flow indexer, mod. 2233 (Lloyd

3 Instruments, UK).

4   A JJ tensile testing machine type T5001 (USA) was used for obtaining the stress-

5 strain curves of the recycled and virgin agricultural plastic pellets used as raw materials,

6 following ISO R527 standard, working at 50 mm/min and at 1 mm/min for elastic

7 modulus determinations. Samples for mechanical testing were prepared in the form of

8 4 mm thick plates by compression molding according to ISO 293 standard, using a

9 hydraulic press (mod. 0-330C, Pasadena Hydraulics Inc., USA).

10   For measuring the length of the RCF, a sample of them was dispersed in water by

11 vigorous stirring. An aliquot was then placed onto a glass slide and dried in a

12 convection oven at 100 ºC for at least 1 h, and finally, the fibers were subjected to

13 image analysis. A macro was specially developed for automatically conducting the

14 measurement of the length of cellulose fibers over 1,600 dpi images obtained by means

15 of a scanner mod. 1640XL (Hewlett-Packard, USA). The images were then analyzed

16 with both Image J (National Institutes of Health, USA) and Leica QWIN (Leica,

17 Germany) software. This method allows the quick measurement of *ca.* 12,000 fibers for

18 each sample, thus obtaining reliable average values. The average length of the cellulose

19 fibers (with standard deviation in brackets) was 583.5 (53.3) μm.

20   For the measurement of the width and thickness of fibers, the scanner resolution

21 (1,600 dpi, which corresponds to *ca.* 16 μm/dot) was not high enough. Hence they were

22 determined over SEM images taken with a JEOL-6610LV field emission scanning

23 electron microscope (Jeol, Japan) at 10 kV. The measurement was done by means of the

24 measuring tool included in the microscope software. Samples were previously sputter-

25 coated with gold to make them conductive prior to SEM observation. Fig. 1 shows a

1 SEM image of the residual cellulose fibers used as reinforcement in this work. Their

2 ribbon-like shape is evidenced, especially for those fibers which lay twisted. Some of

3 the fibers show surface damage, whilst others seem to be fractured; nevertheless, the

4 overall appearance of the fibers is satisfactory, not evidencing a noticeable mechanical

5 degradation due to their processing during Kraft pulping. The resulting average values

6 (with standard deviation in brackets) for both width and thickness of the fibers,

7 determined from several SEM images, are 12.3 (3.0) and 3.5 (0.7) μm, respectively.

8

9 **2.3. Composite preparation**

10 AF200, a recycled plastic in pellet form, obtained from agricultural plastic waste

11 films, was selected as matrix for the composite materials. Composite pellets containing

12 25, 30 and 35 wt% of RCF, without coupling agent and with 1.5 and 3 wt% of MAPE

13 coupling agent, were prepared by compounding the dried raw materials in a Berstorff

14 ZE25 co-rotating intermeshing twin-screw extruder (Germany). Description regarding

15 drying of raw materials and composite pellets can be found in a previous paper

16 (González-Sánchez et al., 2008). Composite pellets obtained were injection molded to

17 obtain ISO 3167 test specimens in a Mateu & Solé reciprocating machine, mod.

18 METEOR 120/45. For obtaining results of wide applicability to different real situations,

19 the general molding principles set by ISO 294-1 standard were followed. The injection

20 molding conditions used are detailed below: Cylinder temperature profiles (four heating

21 zones), which depended on the percentage of fibers, were: 150-155-160-165 ºC for the

22 unreinforced matrix, 170-175-180-185 ºC for composites containing 25 wt% of

23 reinforcement and 175-180-185-188 ºC when 30 wt% of reinforcement was used. For

24 composites containing 35 wt% of reinforcement, the temperature profile also depended

25 on the percentage of coupling agent, being 189-193-197-200 ºC, 184-187-190-193 ºC

1   and 180-183-187-190 ºC the profiles with no coupling agent and with 1.5 and 3 wt% of

2   MAPE coupling agent, respectively. The mold temperature was 50 ºC. Due to the

3   different flow properties of composites (derived from their different composition),

4   cylinder temperature profile, injection rate, as well as injection and holding pressures

5   and times were set for each composite formulation, in order to get a melt viscosity

6   which allowed the filling of the mold in the smoothest way and hence minimized the

7   mechanical attrition and thermal degradation that could arise from the injection molding

8   process. Cavity pressure curves registered on-line were used to adjust molding

9   conditions to the smoothest possible ones for each composite formulation (e.g., such

10   corresponding to the lower pressures which still allow for a complete filling of the

11   mold).

12

13   **2.4. Testing**

14   Both tensile and flexural tests of composites and their corresponding matrices were

15   conducted by means of a universal testing machine (mod. 1011, Instron, USA),

16   following ISO R527 and ISO 178 standards, respectively. Property values reported in

17   Table 3 are the average of measurements made on 6 specimens. Further description of

18   testing conditions can be found in a previous paper (González-Sánchez et al., 2008).

19   Density of molded composites was determined with an XS 105 Dual Range precision

20   scale (METTLER TOLEDO, Switzerland), according to ISO R1183 standard, using

21   method A, which entails the measurement of 3 specimens for each composite.

22   For characterizing the cellulose fibers of the composites, Soxhlet extraction was

23   conducted over composite samples using xylene as solvent. After this step, the analysis

24   method detailed in section 2.2 was followed in order to obtain average values of the

25   length, width and thickness of the fibers.

1

2.5. Scanning electron microscopy

The fractured surfaces of the specimens over which tensile tests at a crosshead rate of 5 mm/min were conducted, were examined using the aforementioned SEM microscope.

3. RESULTS AND DISCUSSION

This section covers the results and discussion regarding the chemical, rheological, thermal and mechanical characterization of the agricultural plastics, the tensile and flexural properties of composites and the reinforcing capability of the residual cellulose fibers used.

3.1 Characterization of the agricultural plastics

The first goal was to characterize the three residual agricultural plastic films for evaluating their degradation level due to their outdoors use. Then, the two recycled agricultural plastic pellets were characterized to evaluate their degradation level as a consequence of their mechanical recycling process. The agricultural virgin plastic characterization was used as additional reference. The experimental results obtained enabled the first evaluation of their suitability as matrices for making cellulose-reinforced composite materials.

3.1.1. Chemical

Fig. 2 shows the FTIR spectra of the three RAPF studied (R1 to R3). The three spectra show the characteristic polyethylene absorptions at 720-730 cm^{-1} (CH$_2$ rocking) and 1460 cm^{-1} (CH$_2$ bending). No other significant bands appear in the spectrum of the

1   sample R2. However, the spectrum of the sample R1 shows that this material contains

2   significant amounts of vinyl acetate moiety, as revealed by the intense bands at

3   1740 cm^{-1} (C=O stretching) and 1240 cm^{-1} (C-O stretching). Small amounts of vinyl

4   acetate also appear in sample R3. Samples R1 and R3 also show broad absorptions

5   between 1000 and 1200 cm^{-1}, revealing the presence of inorganic additives and/or

6   impurities in the residual film.

7   More interesting is the appearance of a weak absorption centered at 1535 cm^{-1} in the

8   spectrum of R1. This band has been assigned to hindered amine light stabilizers, such as

9   Chimassorb 944 (Scoponi et al., 2000). The presence of this band in the waste plastics

10   indicates that significant amounts of photo-stabilizer additives can survive in the plastic

11   after its use, thus increasing the value of the residue.

12   The presence of Chimassorb 944 can be also detected using Ultra-Violet (UV)

13   spectroscopy. Fig. 3 shows the UV spectra of the plastic film wastes. The spectrum of

14   sample R1 shows a clear absorption band centered at 225 nm, which can be assigned to

15   n-π* electronic transitions of 1,3,5-triazine moieties in Chimassorb 944 (Scoponi et al.,

16   2000). Samples R2 and R3 do not show significant absorptions at 225 nm; however, the

17   UV spectra of these samples contain absorption bands centered at about 280 nm, which

18   can be assigned to products generated in the degradation of the plastic during its use.

19   These degradation bands do not appear in the spectrum of R1.

20   The recycled plastic pellets obtained from the RAPF are polyethylene with different

21   amounts of vinyl acetate (VA), photo-stabilizer (and other additives) and degradation

22   products. The FTIR spectrum of AF200 (Fig. 4) shows a strong band at 1740 cm^{-1}

23   corresponding to vinyl acetate. The amount of VA in the recycled plastics, determined

24   by FTIR following the ASTM-D5594-98 (2004) standard, was between 2.5 and 4.5 %.

25   The presence of significant amounts of VA increases the value of the recycled plastic as

1 matrix for cellulose-reinforced composites, since EVA can be used for improving the

2 compatibility between polyethylene and cellulose. The weak band centered at 1535 cm^{-1}

3 reveals the presence of photo-stabilizer, and the weak shoulder observed at 1710 cm^{-1}

4 can be assigned to carbonyl groups generated in the degradation processes.

5 Fig. 5 shows the UV spectra of a virgin plastic (CA2131A) and a recycled plastic

6 (AF200). The main difference appears in the absorption at 225 nm, much more intense

7 in the virgin plastic. Although most of the photo-stabilizer has disappeared during the

8 use, the recycled plastic still contains significant amounts of this valuable additive.

9 Moreover, the recycled plastic shows an absorption band centered at 280 nm,

10 corresponding to degradation products, which do not appear in the virgin plastic.

11

12 *3.1.2. Rheological, thermal and mechanical*

13 Several other properties of the recycled plastics were measured in order to select the

14 most appropriate for being used as matrix for composite materials. Table 2 gives the

15 values of several rheological, thermal and mechanical parameters.

16 In relation to the thermal properties, no significant variation of the melting point

17 was observed when comparing the recycled samples with the virgin one, similarly as it

18 was reported in other works (Chabira et al., 2006; Oreski et al., 2009; Sebaa et al.,

19 1992). In the same way, no increases in the crystallinity were found in the recycled

20 plastics when compared to the virgin one. This result does not agree with the results

21 reported by Chabira et al. (2006). These authors found an increase in crystallinity of

22 degraded LDPE that was assigned to a chemi-crystallization process caused by the

23 photo-degradation. The chemi-crystallization is a process initiated by the thermo- or

24 UV-induced chain scission reactions that take place primarily in the amorphous regions

25 of the polymer during the degradation. The short molecules resulting from chain

1 scissions diffuse to the crystalline regions an join the crystallites, thus increasing the

2 overall crystallinity of the polymer. In our case, the crystallinity increases associated to

3 the degradation were not observed; this result can be explained by considering that the

4 recycled agricultural plastics contain a mixture of different polymers, with different

5 origins, chemical structures and degrees of degradation. Elastic modulus values shown

6 in Table 2 are in good agreement with the measured crystallinities.

7 The Oxidation Induction Time (OIT) values, measured by Differential Scanning

8 Calorimetry, reveal clear differences between the virgin and the recycled plastics. The

9 values measured in the recycled plastics are very much lower due to the severe

10 degradation suffered during their use. Such low OIT values are a serious handicap, as

11 they indicate that the recycled plastics are not suitable for being reprocessed by

12 extrusion and injection molding as they are.

13 Two strategies were evaluated in order to increase the OIT values of the recycled

14 plastics. Firstly, they were mixed with virgin plastics such as CA2131A. However, even

15 a 50/50 mixture of CA2131A and PEBD-IB showed an OIT of only 0.76 minutes, so

16 this strategy was rejected. Better results were obtained when using a phenol-phosphite

17 antioxidant, as with 0.15 wt% of Irganox B900 the OIT measured in AF200 was

18 1.21 min, whereas with 0.3 wt% the OIT increased up to 1.74 min, the latter being

19 considered as sufficient for improving the behavior of the recycled plastic against the

20 oxidative degradation that takes place during the melt compounding process used for

21 obtaining the composites.

22 The mechanical properties of the two recycled plastic pellets are poorer, as

23 expected, than those corresponding to the virgin plastic. The lowest values were

24 measured in PEBD-IB. The elongation at break (ε_{tB}) is severely affected during the

25 degradation, showing a decreasing trend, as it was previously pointed out by Chabira *et*

1 *al.* (2006) and Oreski *et al.* (2009), who also indicated that the dispersion in these

2 breaking values is due to local defects or oxidized spots in the film caused by

3 degradation. This degradation process takes place mainly in the amorphous region,

4 increasing the stiffness of the material (Chabira et al., 2006; Oreski et al., 2009).

5   According to the results shown in Table 2, among the recycled plastics, AF200

6 shows the highest elongation (ε_{tB}) and strength at break (σ_{tB}) values, as well as the

7 greatest OIT, which can also be increased by using the aforementioned phenol-

8 phosphite antioxidant. Therefore, it was chosen as matrix for the composite materials.

9 0.3 wt% of antioxidant was present in both the composites and the matrix blends used

10 as reference.

11

12 **3.2. Composite properties**

13

14 *3.2.1. Tensile*

15   Table 3 gives the mean values (with their corresponding standard deviations in

16 brackets) of the tensile properties measured on composite specimens with different

17 amounts of cellulose fibers and MAPE. As it can be seen, the use of the reinforcement

18 causes remarkable increases in the tensile modulus of elasticity (E_t). With regard to the

19 matrix used, the relative increases registered in E_t for composites without any coupling

20 agent and 25, 30 and 35 wt% of fibers were 392, 525 and 667 %, respectively. E_t

21 experiences a directly proportional increase as the reinforcement content is increased.

22 This suggests that the quality of the fiber dispersion achieved during melt compounding

23 was quite good. The SEM micrographs made at the lowest magnification (1000x)

24 evidence the good fiber dispersion achieved when no coupling agent was present (Fig.

25 7a) and when the coupling agent was used (Figs. 7c and e), as no fiber entanglements

1   can be seen in any case. When dispersion improves, the wetting of the reinforcement by

2   the polymeric matrix also improves, and so does the contact between the matrix and the

3   reinforcement. Fibers partially or completely bonded to the matrix can be closely

4   observed in the magnification corresponding to composites without coupling agent (Fig.

5   7b), thus suggesting a certain degree of wetting. The presence of the polar acetate

6   moiety in the recycled agricultural polyethylene used as matrix would be promoting the

7   observed wetting. This gives rise to an improvement of the matrix-reinforcement stress

8   transfer, which finally results in an increase of the tensile modulus (Kardos, 1991,

9   Karmaker and Youngquist, 1996). Only minor additional increases in E_t were observed

10   when the MAPE coupling agent was used, being 6.5 % the most noticeable increase,

11   achieved for composites containing 35 wt% of fibers and 3 wt% of MAPE. This

12   behavior is due to the fact that the tensile elastic modulus scarcely depends on the

13   quality of the polymer-fiber interphase, since the test in which it is determined involves

14   very low strains (Doan et al., 2006).

15   Table 3 also shows that the use of RCF causes significant increases in the maximum

16   tensile strength (σ_t). Fig. 6 shows the relative maximum tensile strength registered for

17   the composites with regard to that of the matrix used for each composite. The relative

18   increases registered in the maximum tensile strength (σ_t) for composites made without

19   any coupling agent and 25, 30 and 35 wt% of the RCF were 57, 70 and 67 %,

20   respectively. The good results obtained in absence of any added coupling agent can be

21   ascribed to the presence of the polar vinyl acetate moiety of EVA in the recycled

22   agricultural polyethylene used as matrix, which enhances the matrix-reinforcement

23   adhesion to a further extent than the cellulose-thermoplastic mechanical interlocking

24   alone. However, an optimum fiber loading at 30 wt% is observed, which could be

25   ascribed to a poorer dispersion of the reinforcement or to a lower interfacial adhesion as

1 the fiber content is increased, which would lead to a poorer stress transfer from the

2 matrix to the fibers (Ku et al., 2011).

3   As it was mentioned above, the trend shown by the tensile elastic modulus

4 evidenced a good dispersion of the reinforcement in the composites, even for those

5 containing 35 wt% of fibers and no coupling agent. Then, a lower interfacial adhesion

6 as the fiber content is increased is believed to be responsible for the poor stress transfer

7 from the matrix to the fibers. For improving this stress transfer, the interfacial adhesion

8 between fibers and matrix has to be improved. For this purpose, the selected MAPE

9 coupling agent indicated above was used.

10   The increases registered in the relative maximum tensile strength of the composites

11 containing MAPE suggest an improvement of the interfacial adhesion. In order to

12 ascertain the validity of this hypothesis, the morphology of the composites was studied

13 using SEM. Fig. 7 shows typical SEM images of fractured surfaces of the composites

14 studied in this work. The magnified micrograph corresponding to composites made

15 without coupling agent (Fig. 7b) shows that some fibers are pulled out from the matrix

16 during the fracture, revealing a poor interfacial adhesion. Fig. 7b also shows fibers that

17 are broken, rather than pulled out, as corresponds to the presence of the polar vinyl

18 acetate moiety of EVA that promotes the wetting of the fibers and the adhesion. When

19 1.5 wt% of MAPE is used (Fig. 7d), the appearance of voids decreases and most of the

20 cellulose fibers are broken (rather than pulled out) at the fracture surface, thus showing

21 an improvement of the interfacial adhesion. With a further increase in MAPE

22 concentration (up to 3 wt%), the latter effect appears to be extended (Fig. 7f). Moreover,

23 the occurrence of some ductile fractures reveals that the matrix has been deformed

24 before the fibers embedded in those places were finally broken, which is a clear sign of

25 the improvement of the stress transfer from the matrix to the fibers. Table 3 also shows

1   some increased tensile strain at break values for composites containing MAPE, such as

2   the increase observed for 35 wt%-reinforced composites containing 3 wt% of MAPE

3   with regard to 35 wt%-reinforced composites with no coupling agent.

4   However, while evidences of the improvement of interfacial adhesion have been found,

5   the enhancement of the tensile strength observed for composites containing MAPE

6   reach a maximum of 12.4 %, when comparing the relative maximum tensile strengths

7   calculated for composites containing 35 wt% of reinforcement and 3 wt% of MAPE

8   with composites with the same fiber loading and no coupling agent. To ascertain the

9   reasons of the observed behavior, fibers from the three composites with 35 wt% of

10 reinforcement and 0, 1.5 and 3 wt% of MAPE were Soxhlet extracted from composites

11 and studied by the image analysis method detailed in section 2.2, which entails the

12 measurement of *ca.* 12,000 fibers for each sample. Average lengths obtained by this

13 way are shown in Table 4. Average fiber length decreased as the MAPE content is

14 increased. Hence, when 1.5 wt% of MAPE was used, the average fiber length decreased

15 8.1 % with regard to the composites without coupling agent, whereas for composites

16 with 3 wt% of MAPE the reduction reached 15.0 %. In terms of aspect ratio (L/D),

17 reductions were, respectively, of 10.9 % and 13.8 %, thus evidencing that fiber attrition

18 cannot be neglected. This phenomenon, which would be reducing the tensile properties

19 of the fibers, can be ascribed to an increase in shear forces undergone by the fibers as a

20 consequence of their chemical bonding with the matrix, in accordance with the results

21 obtained by Vilaseca et al. (2010) when studying the effect of a maleated polypropylene

22 over tensile properties of abaca strand-reinforced polypropylene composites.

23 Furthermore, in view of the degree of reduction of average fiber length, the shorter fiber

24 fragments resulting from fiber breakage would possibly be acting as filler instead of as

25 reinforcement.

1   On the other hand, the use of MAPE leads to a reduction of the tensile strength of

2   the matrix as it can be seen in the values obtained when no reinforcement is used. This

3   is believed to be due to the plasticizing effect of MAPE, as a consequence of its lower

4   average molecular weight. This phenomenon can also be assumed to happen in

5   composites, where some MAPE may remain freely dispersed, not contributing to the

6   fiber/matrix adhesion (Ku et al., 2011). Hence, both fiber length reduction and the

7   plasticizing effect, which occur when increasing MAPE content, are considered as

8   responsible for the absence of a noticeable enhancement of tensile properties although

9   an improvement of the interfacial adhesion was evidenced.

10

11   *3.2.2. Flexural*

12   The flexural properties of the composites studied in this work are also shown in

13   Table 3. These composites did not break during the flexural tests and, therefore, the

14   flexural strength was determined at a deflection of 6 mm, according to ISO 178

15   standard. Both the flexural elastic modulus (E_f) and the flexural strength (at 6 mm

16   deflection – $\sigma_{f\text{-}6mm}$) of composites considerably improve by increasing the RCF content.

17   Thus, with regard to the matrix used, the relative increases registered in E_f for

18   composites without coupling agent and 25, 30 and 35 wt% of fibers were 558, 750 and

19   892 %, respectively; while for those fiber contents, $\sigma_{f\text{-}6mm}$ increased by 216, 286 and

20   322 %. The use of the MAPE coupling agent does not give rise to great improvements

21   in E_f values, which can be ascribed to the same aforementioned considerations when

22   assessing E_t results. Nevertheless, for composites containing 35 wt% of RCF, the use of

23   3 wt% of MAPE led to a 10.9 % improvement in E_f.

24   As for the influence of the addition of a coupling agent on the flexural strength at 6

25   mm deflection, no noticeable effect can be observed for composites with 25 and 30 wt%

1 of reinforcement, while for those with 35 wt% a moderate increase (up to 11.1 % when

2 3 wt% of MAPE was added) was evidenced. This behavior could be explained

3 considering two conflicting phenomena which take place when using MAPE. On one

4 hand, the interfacial adhesion is improved (as evidenced in SEM images), so that the

5 stress transfer will also improve, leading to a stronger polymer-fiber interphase. On the

6 other hand, as shown in Table 4, the length of the fibers decreases as the MAPE

7 coupling agent content increases. This would be contributing to a reduction of the

8 strength of the composite. In view of the results obtained, when 35 wt% of RCF is used,

9 the enhancement of the interfacial adhesion provided by the MAPE coupling agent

10 appears to be the dominant effect, which is reflected in the registered improvement of

11 flexural strength.

12

13 ### 3.3. Reinforcing capability of the residual cellulose fibers

14 The reinforcing capability of the fibers depends on their intrinsic mechanical

15 properties and is a key factor for obtaining composites with improved performance and

16 for a deeper understanding of composite properties. However, very few data regarding

17 intrinsic properties can be found for *Eucaliptus* Kraft-pulped fibers, despite they are one

18 of the most abundant cellulose pulp fibers. The reason stems in their short length, which

19 only allows for the estimation of their intrinsic properties by indirect means.

20 As known, the tensile elastic modulus of composites (E_c) can be predicted by

21 several models. After a comparative study, Facca et al. (2006) concluded that the most

22 accurate model for natural fiber reinforced composites was that of the semi-empirical

23 Halpin-Tsai equation, which, when applied to the determination of tensile elastic

24 modulus of composites, takes the following form (Halpin and Kardos, 1976):

25
$$E_i = E_m \frac{1 + \xi \eta_i V_r}{1 - \eta_i V_r} \quad (2)$$

1   being

$$\eta_i = \frac{\dfrac{E_r}{E_m} - 1}{\dfrac{E_r}{E_m} + \xi} \quad (3)$$

3   where V_r is the volume fraction of the reinforcement, E_i is the tensile modulus of the

4   composite for the corresponding loading conditions (i can be 1 when calculating the

5   longitudinal modulus, or 2 when calculating the transverse modulus), and E_r and E_m are

6   the tensile elastic moduli of the reinforcement and the matrix, respectively. ξ, the

7   Halpin-Tsai parameter, must be related to reinforcement geometry (aspect ratio) and

8   depends on loading conditions. Thus, it can be estimated as (Halpin and Kardos, 1976):

9    $$\xi = 2\left(\frac{a}{b}\right) \quad (4)$$

10   For 2D randomly oriented short fiber composites, like those corresponding to the

11   injection molding specimens obtained in this work, the following averaging technique

12   can be used in the estimation of E_c (Fu et al., 2009):

13    $$E_c = \frac{3}{8}E_1 + \frac{5}{8}E_2 \quad (5)$$

14   where E_1 and E_2 stand for the longitudinal and transversal tensile moduli,

15   respectively, which can be calculated by using the Halpin-Tsai equation.

16   For a longitudinal loading direction the "a" and "b" terms of the ξ parameter stand for

17   the average length and diameter of the fibers, while for a transverse loading direction,

18   they stand for the average width and thickness of the fibers. Hence, an equivalent

19   diameter was calculated in order to assume the ribbon shape fibers as cylindrical ones.

20   The equivalence was done so that the resulting cylindrical fibers had the same length

21   and the same surface in contact with the matrix (interfacial area) than the ribbon shaped

22   ones (neglecting both fiber ends). According to this assumptions, the values of the ξ

1   parameter would be $2 \cdot (L/D)_{av}$ and 2 for longitudinal and transverse loading directions,

2   respectively. Table 4 shows average values of the length, the width, the thickness, the

3   surface-based equivalent diameter and the subsequent equivalent aspect ratios of the

4   fibers for the different MAPE contents.

5   V_r was calculated from the mass fraction of reinforcement (θ_r), the experimental

6   density of composites (ρ_c) and the density of reinforcement (ρ_r). ρ_r was calculated by

7   using the *rule of mixtures* given by the equation 6 applied to the experimental ρ_c values

8   given in Table 3:

9    $$\frac{1}{\rho_c} = \frac{1}{\rho_m} + \left(\frac{1}{\rho_r} - \frac{1}{\rho_m} \right) \cdot \theta_r \qquad (6)$$

10   The values of ρ_r, calculated for each MAPE content, are shown in Table 4, as well

11   as those of the R-square parameter. The almost perfect linear fitting of the experimental

12   density data reveals the reliability of the calculated ρ_r values, as well as the dosing of

13   raw materials during the extrusion and the injection molding processing, as no voids

14   appear to have remained within the specimens.

15   According to the calculated data and the Halpin-Tsai equations, the theoretical

16   values of E_c were estimated by a trial and error method which iteratively assumes the

17   value of E_r which minimizes the average-square error between the experimental and the

18   theoretical values of E_c. Fig. 8 shows both the experimental and the theoretical values of

19   E_c. It can be observed that in the range of V_r studied, the calculated and the experimental

20   values fit adequately. Table 4 shows the calculated values of E_r for each MAPE content.

21   Bearing in mind the residual character of the *Eucalyptus* Kraft-pulped fibers used in this

22   work as well as their attrition during extrusion compounding and injection molding, the

23   average intrinsic tensile modulus determined for them (16.4 GPa) may be deemed as

24   consistent with that determined by Neagu et al. (2006) for virgin *Eucaliptus* Kraft-

pulped fibers from European sources (30.7 GPa). Despite their residual origin, they are

a suitable reinforcement for increasing the stiffness of composites, since their intrinsic

tensile elastic modulus is 109 to 143 times that shown by the polymeric matrix.

On the other hand, the intrinsic tensile strength of the RCF used was also estimated

by means of a modified rule of mixtures according to the model developed by Fu and

Lauke (1996), which is often used to predict the tensile strength of short-fiber

composites:

$$\sigma_c = \chi_1\chi_2\sigma_rV_r+(1-V_r)\sigma_m \quad (7)$$

where χ_1 is the fiber orientation factor, χ_2 is the fiber length factor, σ_c and σ_r are the

ultimate strengths of the composite and the fibers, respectively, and σ_m is the matrix

stress at the failure of the composite. As both χ_1 and χ_2 are dependent on each other, it is

more useful to work with their product ($\chi_1\chi_2$) which is known as the *fiber efficiency*

factor for the strength of the composite, and represents the efficiency of the stress

transfer between matrix and reinforcement. Thus, the value chosen for the fiber

efficiency factor ($\chi_1\chi_2$) was the one given for composites with a 2D random distribution,

like those corresponding to the injection molded specimens obtained in this work,

namely 0.417 (Fu et al., 2009).

V_r values were calculated as described previously. σ_m was calculated assuming that

the failure of the matrix takes place at the same strain as that of the composite. Then, a

polynomial fitting of the averaged curve obtained from the stress-strain curves

corresponding to the 6 specimens tested for each material was done.

The value of σ_r estimated by means of this model must be considered as an overall

contribution of the fibers to the tensile strength of the composite, or as a measure of the

apparent intrinsic tensile strength of the reinforcement, but not as the real tensile

strength of the fibers.

1   Fig. 9 shows the calculated values of σ_r for each composite. As it can be seen, the

2   estimated intrinsic tensile strength is lower as the fiber loading increases. This can be

3   ascribed to the fact that with bigger amounts of reinforcement, the fiber length will

4   decrease, and also there will be more fiber-fiber interactions. When the MAPE is used,

5   the two aforementioned conflicting phenomena will take place. That is the interfacial

6   adhesion improvement, which leads to a stronger polymer-fiber interphase and the

7   decrease of fiber length, which reduces their reinforcing ability. From Fig. 9 it can be

8   concluded that when 1.5 wt% of MAPE is added, the first phenomenon is weaker than

9   the second one, since σ_r decreases for every fiber content. However, when the MAPE

10   content is increased to 3 wt%, the trend is smoothed for composites containing 30 wt%

11   of fibers, while it is inverted for composites with 25 and 35 wt% of reinforcement.

12   Nevertheless, the use of coupling agent only leads to an improvement of σ_r when 3 wt%

13   of MAPE is added to composites with 35 wt% of reinforcement.

14   Overall, the estimated intrinsic tensile strength of the residual cellulose fibers used

15   as reinforcement in this work ranges from 161.6 to 198.4 MPa, which is 14.0 to 17.2

16   times higher than that shown by the neat recycled agricultural plastic, thus revealing

17   their value as reinforcement.

18

19   **4. CONCLUSIONS**

20   Plastic wastes from modern intensive agriculture and residual cellulose fibers from

21   Kraft pulping processes have successfully been used for obtaining environmentally

22   sustainable and cost-effective eco-composites through an extrusion-compounding

23   technology at pilot plant scale. Even when no coupling agent was used, the maximum

24   tensile strength of composites increased up to 70 %, with regard to that of the matrix, in

25   consequence of the enhanced matrix-reinforcement compatibility provided by the polar

1 vinyl acetate moiety of the EVA that was found to be present in the recycled plastic

2 used as matrix. The presence of significant amounts of EVA and photo-stabilizer in the

3 recycled plastic increases its value as matrix for cellulose-reinforced composites. The

4 addition of the maleic anhydride-modified polyethylene coupling agent improves the

5 interfacial adhesion but also causes a fiber length reduction and a plasticizing effect.

6 These three effects explain the moderate tensile strength enhancements achieved when

7 using the coupling agent. The reinforcing capability of the *Eucalyptus Globulus* residual

8 fibers was also estimated through the fitting of the experimental results to

9 micromechanical models, thus providing scientific data to literature regarding properties

10 hitherto scarcely available. The estimated properties revealed the potential of these

11 wastes as reinforcement for several kinds of eco-composites. The properties of the eco-

12 composites obtained from residual cellulose and recycled agricultural plastics enable

13 their immediate use in numerous industrial applications, thus preventing waste

14 generation.

15

23

24 **REFERENCES**

1   [1] Abdel-Bary, E.M., Ismail, M.N., Yehia, A.A., Abdel-Hakim, A.A., 1998. Recycling

2   of polyethylene films used in greenhouses – development of multilayer plastic films.

3   Polym. Degrad. Stab. 62, 111-115.

4   [2] Abdelmouleh, M., Boufi, S., Belgacem, M.N., Dufresne, A., 2007. Short

5   natural-fiber reinforced polyethylene and natural rubber composites: Effect of silane

6   coupling agents and fibers loading. Compos. Sci. & Technol. 67, 1627-1639.

7   [3] Arrakhiz, F.Z., El Achaby, M., Malha, M., Bensalah, M.O., Fassi-Fehri, O.,

8   Bouhfid, R., Benmoussa, K., Qaiss, A., 2013. Mechanical and thermal properties of

9   natural fibers reinforced polymer composites: Doum/Low density polyethylene. Mat.

10 and Des. 43, 200-205.

11 [4]   Bledzki, A.K., Gassan, J., 1999. Composites reinforced with cellulose based

12 fibers. Prog. Polym. Sci. 24, 221-274.

13 [5] Cajaraville, J.E., Galarza, L.Z., Vicente, S., 2010. Cultivos protegidos en China

14 (*Protected crops in China*). Market Study, Business Center Office of Madrid's

15 Commonwealth, Madrid.

16 [6]   Chabira, S.F., Sebaa, M., Huchon, R., De Jeso, B., 2006. The changing anisotropy

17 character of weathered low-density polyethylene films recognized by quasi-static and

18 ultrasonic mechanical testing. Polym. Degrad. Stab. 9, 1887-1895.

19 [7]   de la Orden MU, González Sánchez C, González Quesada M, Martínez Urreaga J.,

20 2007. Novel polypropylene-cellulose composites using polyethylenimine as coupling

21 agent. Compos: Part A. Appl. Sci. Manuf. 38(9), 2005-2012.

22 [8] Department of Agriculture, Food and Environment of Spain, 2012. Encuestas sobre

23 superficies y rendimientos de cultivos *(Crops yields and surfaces survey)*, Madrid.

24 [9]   Doan, T-T-L., Gao, S-L., Mäder, E., 2006. Jute/polypropylene composites I.

25 Effect of matrix modification. Comp. Sci. Technol. 66, 952-963.

1   [10] Facca, A.G., Kortschot, M.T., Yan, N., 2006. Predicting the elastic modulus of

2   natural fibre reinforced thermoplastics. Compos: Part A. Appl. Sci. Manuf. 37, 1660-

3   1671.

4   [11] Fu, S-Y., Lauke, B., 1996. Effects of fiber length and fiber orientation

5   distributions on the tensile strength of short-fiber-reinforced polymers. Compos. Sci.

6   Technol. 56, 1179-1190.

7   [12] Fu, S-Y., Lauke, B., Mai, Y-W., 2009. Science and engineering of short fibre

8   reinforced polymer composites. Woodhead Publishing and CRC Press, Boca Raton.

9   [13] González-Sánchez C, González-Quesada M, de la Orden MU, Martínez Urreaga

10   J., 2008. Comparison of the effects of polyethylenimine and maleated polypropylene

11   coupling agent onto the properties of cellulose-reinforced polypropylene composites. J.

12   Appl. Polym. Sci. 110(5), 2555-2562.

13   [14] Halpin, J.C., Kardos, J.L., 1976. The Halpin-Tsai Equations: A Review. Polym.

14   Engin. Sci. 16(5), 344-352.

15   [15] Hussain, I., Hamid, H., 2003. Plastics in agriculture, in: Andrady, A.L. (Ed.),

16   Plastics and the Environment. John Wiley and Sons, New York, p. 185.

17   [16] Kardos, J.L., 1991. Mechanical properties of polymeric composite materials, in:

18   Baer, E., Moet, A. (Eds.), High performance polymers: Structure, properties,

19   composites, fibers. Carl Hanser Verlag, Munich, pp. 199-241.

20   [17] Karmaker, A.C., Youngquist, J.A., 1996. Injection molding of polypropylene

21   reinforced with short jute fibers. J. Appl. Polym. Sci. 62, 1147-1151.

22   [18] Ku, H., Wang, H., Pattarachaiyakoop, N., Trada, M., 2011. A review on the tensile

23   properties of natural fiber reinforced polymer composites. Compos: Part B.

24   Engineering. 42, 856-873.

1 [19] Neagu, R.C., Gamstedt, E.K., Berthold, F., 2006. Stiffness contribution of various

2 wood fibers to composite materials. J. Compos. Mater. 40(8), 663-699.

3 [20] Oreski, G., Wallner, G.M., Lang, R.W., 2009. Ageing characterization of

4 commercial ethylene copolymer greenhouse films by analytical and mechanical

5 methods. Biosyst. Engin. 103, 489-496.

6 [21] Plastics Europe, 2011. Plastics – the Facts 2011, Brussels.

7 [22] Plastics Europe, 2012. Plastics – the Facts 2012, Brussels.

8 [23] Scaffaro, R.; Tzankova, N.; La Mantia, F.P., 2006. On the effectiveness of

9 different additives and concentrations on the re-building of the molecular structure of

10 degraded polyethylene. Polym. Degrad. 91, 3110-3116.

11 [24] Scoponi, M., Cimmino, S., Kaci, M., 2000. Photo-stabilization mechanism under

12 natural weathering and accelerated photo-oxidative conditions of LDPE films for

13 agricultural applications. Polymer 41, 7969-7980.

14 [25] Sdrobiş, A., Darie, R.N., Totolin, M., Cazacu, G., Vasile, C., 2012. Low density

15 polyethylene composites containing cellulose pulp fibers. Comp. Part B. 43, 1873-1880.

16 [26] Sebaa, M., Servens, C., Pouyet, J., 1992. Natural and artificial weathering of low-

17 density Polyethylene (LDPE): Calorimetric analysis. J. Appl. Polym. Sci. 45, 1049-

18 1053.

19 [27] Sunilkumar, M. Francis, T., Thachil, E.T., Sujith, A., 2012. Low density

20 polyethylene–chitosan composites: A study based on biodegradation. Chem. Eng. J.

21 204–206, 114–124.

22 [28] Vilaseca, F., Valadez-González, A., Herrera-Franco, P.J., Pèlach, M.A., López,

23 J.P., Mutjé, P., 2010. Biocomposites from abaca strands and polypropylene. Part I:

24 Evaluation of the tensile properties. Bioresour. Technol. 101, 387-395.

25

1 **FIGURE CAPTIONS**

2 Fig. 1. SEM micrograph of isolated residual cellulose fibers.

3

4 Fig. 2. FTIR spectra of the three agricultural plastic film wastes studied.

5

6 Fig. 3. UV spectra of the three agricultural plastic film wastes studied.

7

8 Fig. 4. FTIR spectrum of AF200

9

10 Fig. 5. UV spectra of a virgin agricultural plastic (CA2131A, solid line) and a recycled

11 one (AF200)

12

13 Fig. 6. Effects of fiber and coupling agent contents on the relative maximum tensile

14 strength of composites containing recycled agricultural plastic AF200 and residual

15 cellulose fibers.

16

17 Fig. 7. SEM micrographs of fractured surfaces of recycled agricultural plastic AF200-

18 residual cellulose-fiber composites: (a and b) without coupling agent, (c and d) with

19 1.5 wt% MAPE, (e and f) with 3 wt% MAPE.

20

21 Fig. 8. Experimental and theoretical values of the tensile elastic modulus of composites

22 containing recycled agricultural plastic AF200 and residual cellulose fibers.

23

24 Fig. 9. Estimated values of the tensile strength of the residual cellulose fibers for

25 different fiber and MAPE contents, according to the modified rule of mixtures.

26

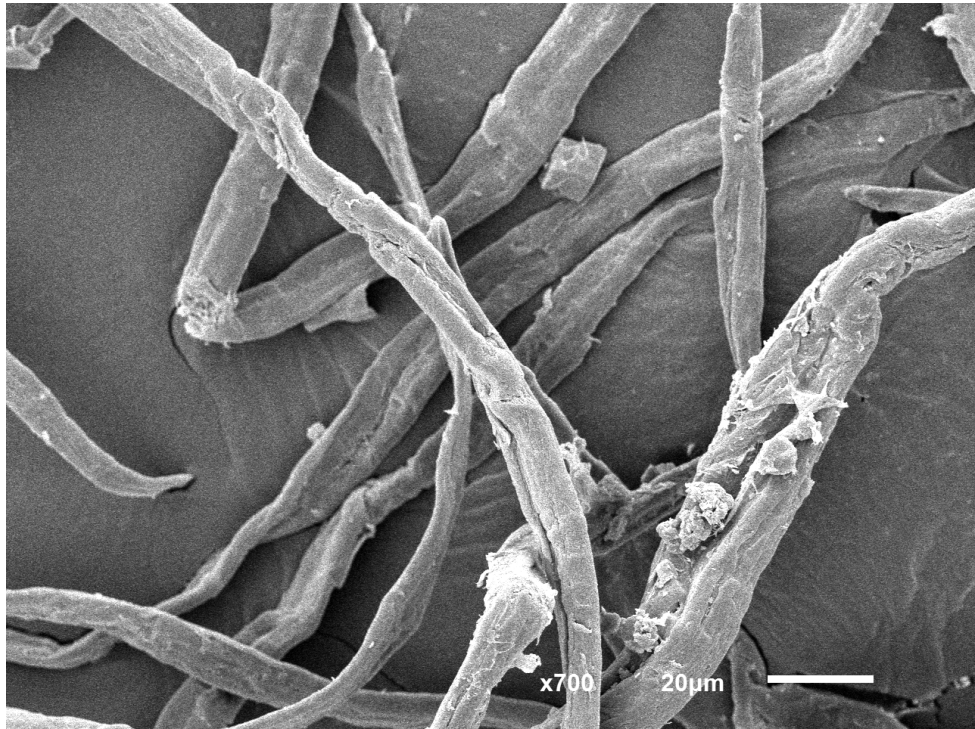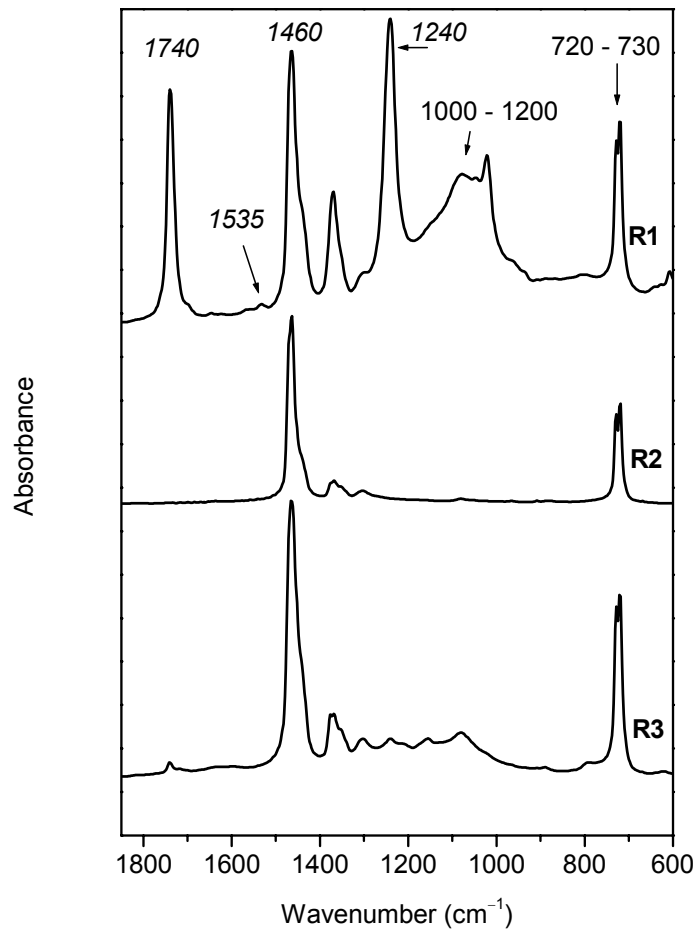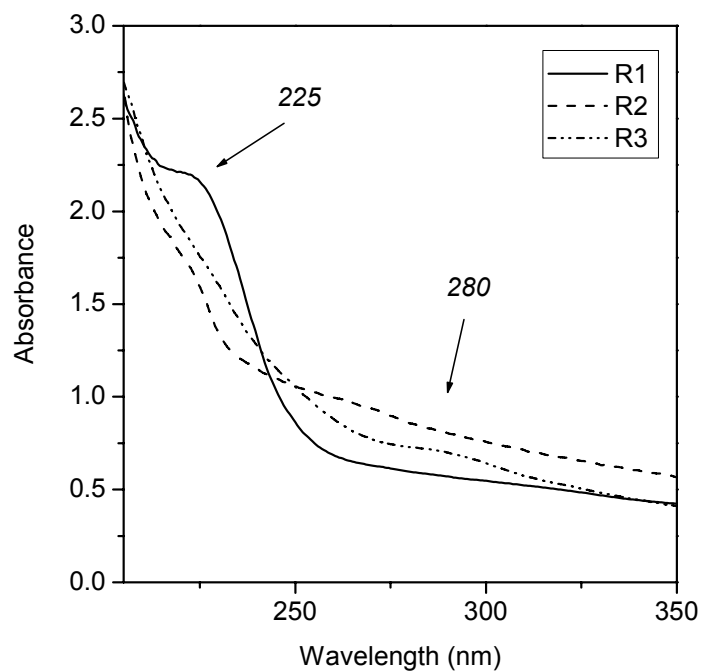1   Fig. 1. SEM micrograph of isolated residual cellulose fibers.

2

13

1   Fig. 2. FTIR spectra of the three agricultural plastic wastes studied.
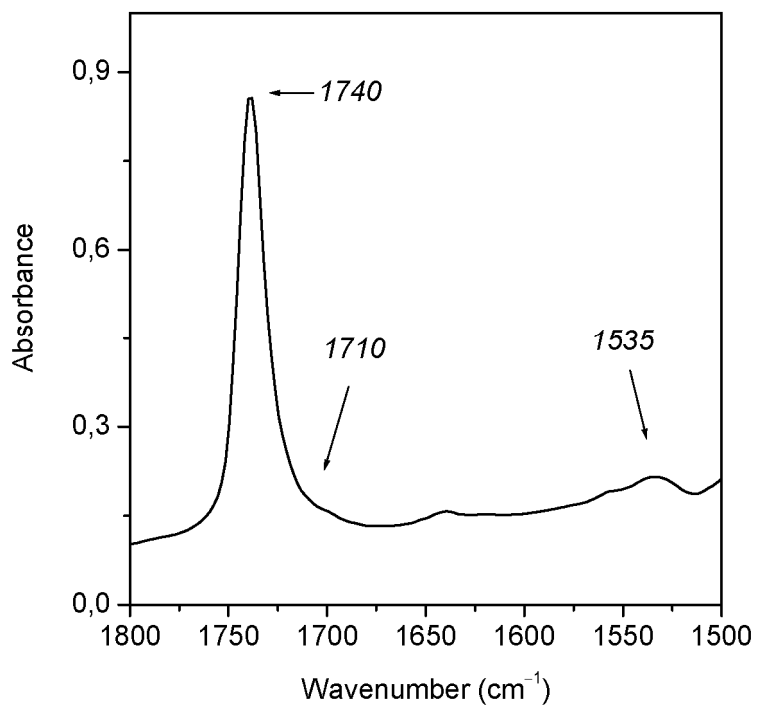
2

1   Fig. 3. UV spectra of the three agricultural plastic film wastes studied.
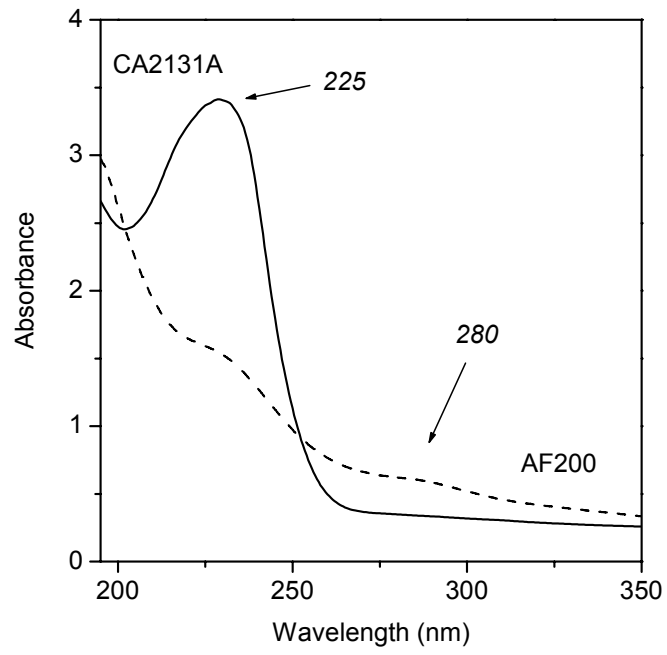

2

3

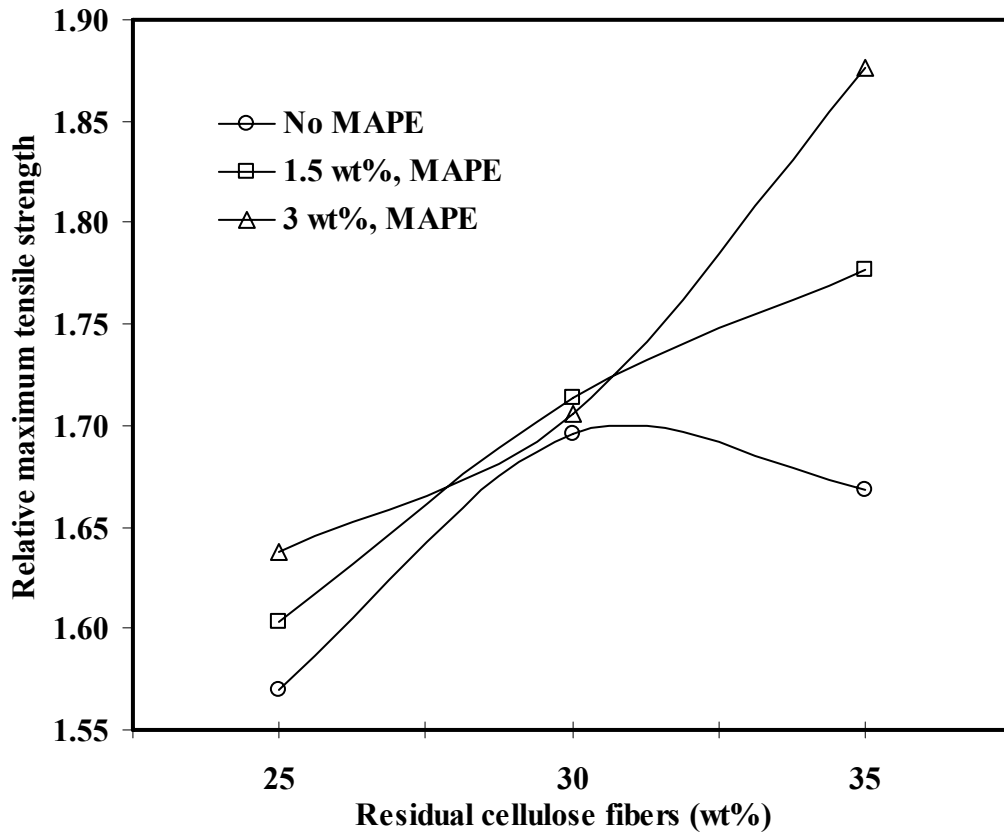1   Fig. 4. FTIR spectrum of AF200

2

3

1 Fig. 5. UV spectra of a virgin agricultural plastic (CA2131A, solid line) and a recycled

2 one (AF200)

3

4

1   Fig. 6. Effects of fiber and coupling agent contents onto the relative maximum tensile

2   strength of composites containing recycled agricultural plastic AF200 and residual
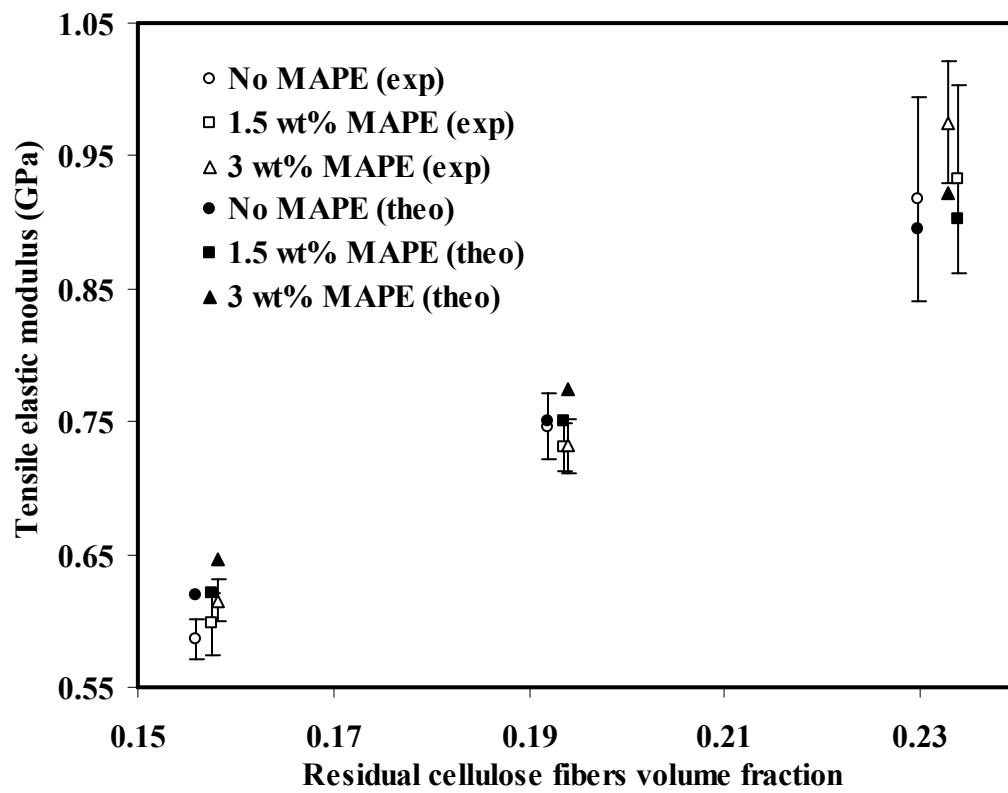
3   cellulose fibers

4

5

1   Fig. 7. SEM micrographs of fractured surfaces of recycled agricultural plastic AF200-

2   residual cellulose-fiber composites: (a and b) without coupling agent, (c and d) with

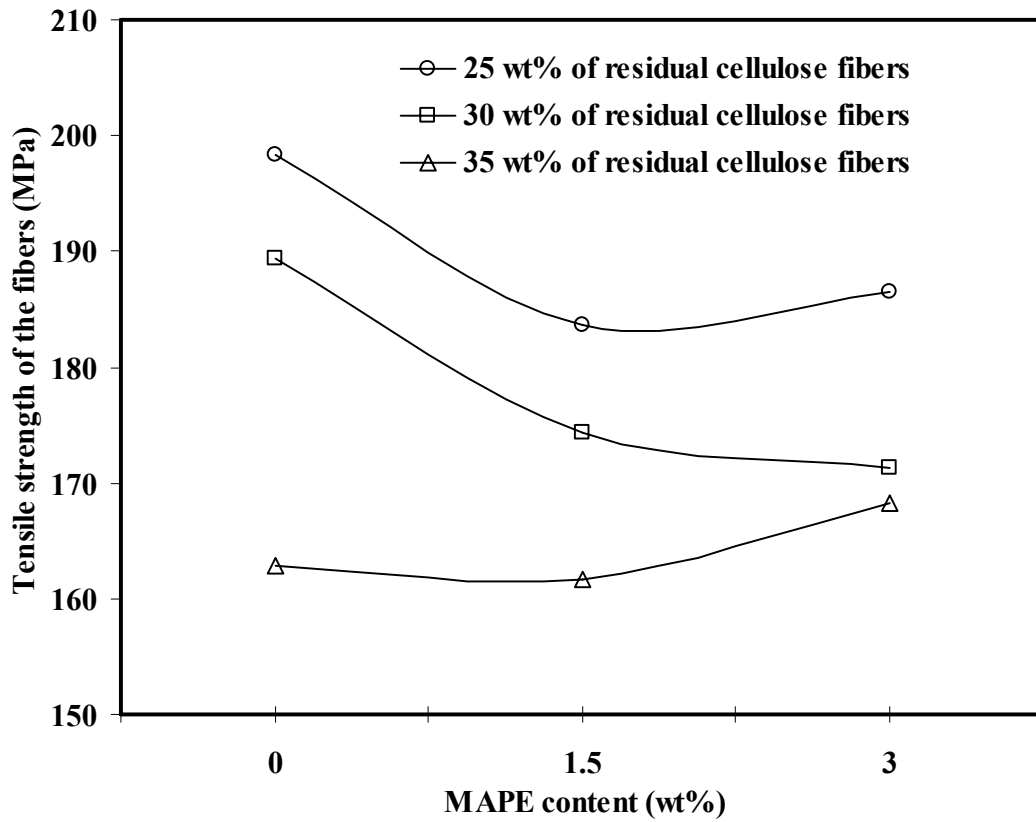3   1.5 wt% MAPE, (e and f) with 3 wt% MAPE.

4
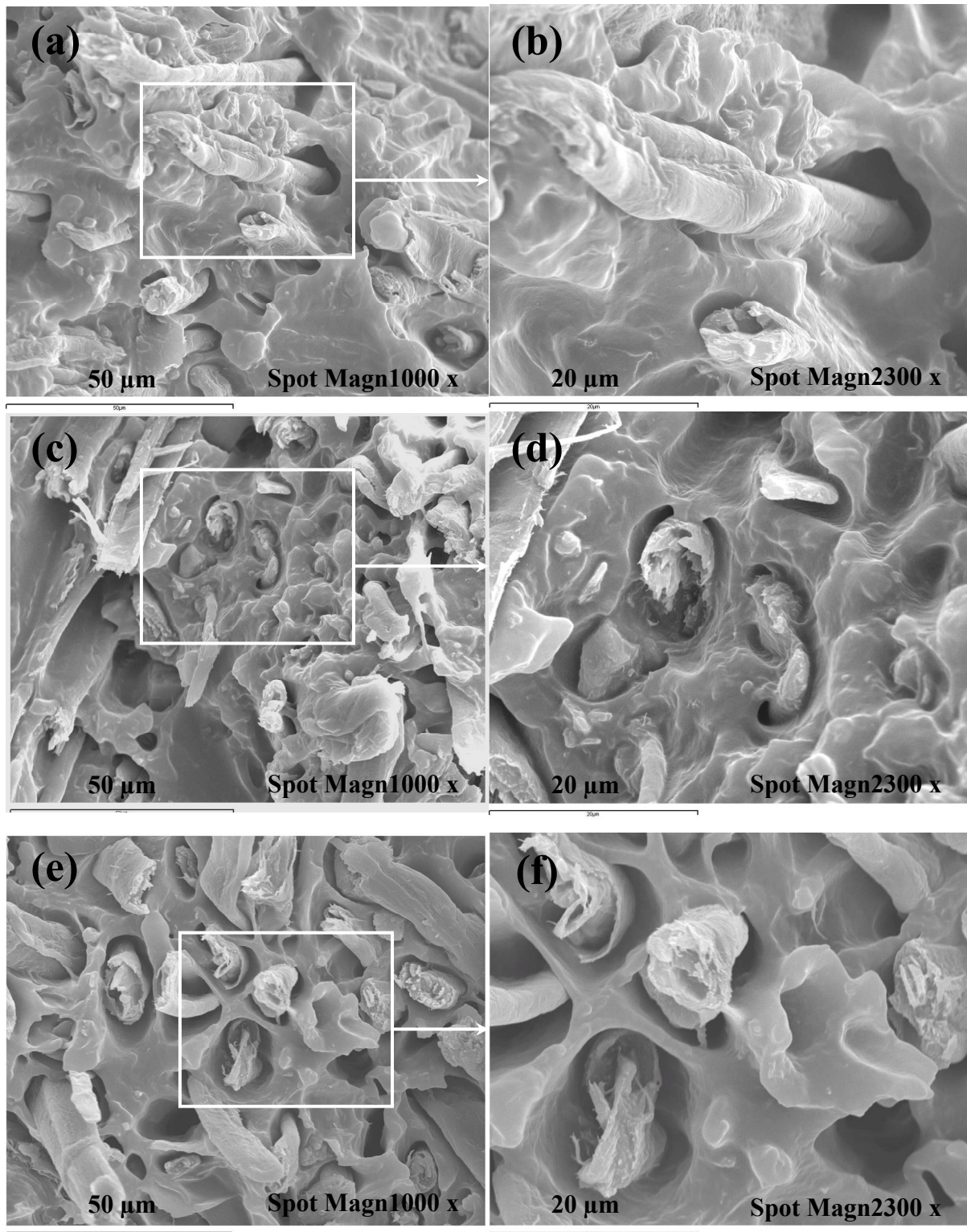
1   Fig. 8. Experimental and theoretical values of the tensile elastic modulus of composites

2   containing recycled agricultural plastic AF200 and residual cellulose fibers.

3

4

1   Fig. 9. Estimated values of the tensile strength of the residual cellulose fibers for

2   different fiber and MAPE contents, according to the modified rule of mixtures.

3

1   **TABLES**

2

3   Table 1. Characteristics of the recycled and virgin agricultural plastic pellets used in this

4   study, provided by the suppliers.

5

6   Table 2. Characteristics of the recycled and virgin agricultural plastic pellets,

7   determined in this study.

8

9   Table 3. Mechanical properties and density of composites containing recycled

10   agricultural plastic AF200 and residual cellulose fibers.

11

12   Table 4. Average length (L_{av}), width (w_{av}), thickness (th_{av}), equivalent diameter (D_{av}),

13   aspect ratio ($(L/D)_{av}$), density (ρ_r) and intrinsic tensile modulus (E_r) of the residual

14   cellulose fibers.

15

1   Table 1. Characteristics of the recycled and virgin agricultural plastic pellets used in this

2   study, provided by the suppliers.

Material	MFI (190 ºC, g/10 min)	Density (g/cm^3)	Colour
AF200	0.19-0.56	0.935	Brownish
PEBD-IB	0.2-0.3	-	Brown
CA2131A	0.4	0.947	White

3

4

1 Table 2. Characteristics of the recycled and virgin agricultural plastic pellets,

2 determined in this study.

Material	MFI (g/10 min) (at 190 ºC)	Melting point (ºC)	Crystallinity (%)	OIT (min)	E_t (MPa)	ε_{tB} (%)	σ_{tB} (MPa)
AF200	0.35	109.7	33.3	0.81	110.28 (2.78)	697.7 (23.60)	12.66 (0.06)
PEBD-IB	0.22	112.6	33.7	0.55	118.81 (3.34)	78.50 (14.66)	8.81 (0.09)
CA2131A	0.37	112.4	40.7	>120	128.01 (3.71)	809.9 (17.56)	14.34 (0.68)

3

4

1   Table 3. Mechanical properties and density of composites containing recycled

2   agricultural plastic AF200 and residual cellulose fibers.

Reinforcement (wt%)	MAPE (wt%)	ρ_c (g/cm³)	E_t (GPa)	σ_t (MPa)	ε_{tB} (%)	E_f (GPa)	$\sigma_{f\text{-}6mm}$ (MPa)
0		0.931 (0.000)	0.12 (0.01)	11.56 (0.55)	121.50 (3.80)	0.12 (0.01)	5.11 (0.32)
25	0	1.046 (0.002)	0.59 (0.01)	18.15 (0.17)	9.86 (0.40)	0.79 (0.05)	16.15 (0.33)
30		1.073 (0.002)	0.75 (0.03)	19.61 (0.14)	7.73 (0.32)	1.02 (0.03)	19.72 (0.14)
35		1.100 (0.001)	0.92 (0.08)	19.29 (0.55)	6.09 (0.32)	1.19 (0.04)	21.57 (0.40)
0		0.933 (0.000)	0.12 (0.00)	10.96 (0.27)	109.70 (4.30)	0.17 (0.01)	4.39 (0.03)
25	1.5	1.046 (0.001)	0.60 (0.02)	17.57 (0.12)	10.21 (0.28)	0.78 (0.03)	16.09 (0.14)
30		1.071 (0.001)	0.73 (0.02)	18.78 (0.21)	8.07 (0.17)	0.93 (0.06)	18.87 (0.21)
35		1.109 (0.001)	0.93 (0.07)	19.47 (0.60)	5.87 (0.67)	1.28 (0.07)	22.87 (0.15)
0		0.933 (0.000)	0.14 (0.01)	10.80 (0.07)	117.90 (2.70)	0.15 (0.01)	5.53 (0.03)
25	3	1.049 (0.001)	0.62 (0.02)	17.69 (0.11)	9.99 (0.47)	0.80 (0.02)	16.43 (0.10)
30		1.071 (0.002)	0.73 (0.02)	18.42 (0.18)	7.64 (0.38)	1.08 (0.08)	19.59 (0.23)
35		1.102 (0.000)	0.98 (0.05)	20.26 (0.32)	6.33 (0.39)	1.32 (0.05)	23.96 (0.16)

3

4

1   Table 4. Average length (L_{av}), width (w_{av}), thickness (th_{av}), equivalent diameter (D_{av}),

2   aspect ratio (($L/D)_{av}$), density (ρ_r) and intrinsic tensile modulus (E_r) of the residual

3   cellulose fibers.

4

MAPE (wt%)	L_{av} (µm)	w_{av} (µm)	th_{av} (µm)	D_{av} (µm)	$(L/D)_{av}$	ρ_r (g/cm^3)	R^2	E_r (GPa)
0	504.0 (32.0)	11.39 (2.47)	3.56 (0.63)	9.51	53.0	1.676	1.0000	16.7
1.5	463.3 (44.4)	12.39 (2.88)	3.12 (0.40)	9.87	46.9	1.659	0.9978	17.2
3	428.6 (18.2)	11.44 (2.87)	3.27 (0.91)	9.37	45.7	1.657	0.9995	15.2

5